Feasibility Study of Tokamak, Helical and Laser Reactors as Affordable Fusion Volumetric Neutron Sources

T. Goto[1,2], T. Tanaka[1,2], H. Tamura[1,2], J. Miyazawa[1,2], A. Iwamoto[1,2], N. Yanagi[1,2], T. Fujita[3], R. Kodama[4], Y. Mori[5]

[1] National Institute for Fusion Science (NIFS), National Institutes of Natural Sciences (NINS), Toki, Gifu, 509-5292, Japan
[2] The Graduate University for Advanced Studies, Toki, Gifu, 509-5292, Japan
[3] Nagoya University, Nagoya, 464-8603, Japan
[4] Institute of Laser Engineering, Osaka University, Suita, Osaka, 565-0871, Japan
[5] The Graduate School for the Creation of New Photonics Industries, Hamamatsu, Shizuoka, 431-1202, Japan

E-mail: goto.takuya@nifs.ac.jp

Abstract

The applicability of tokamak, helical and laser fusion reactors as a volumetric fusion neutron source has been examined using the systems codes that have been utilised for the conceptual design of DEMO and commercial reactors in Japan. This study has clarified the characteristics of reactor-based volumetric neutron sources that can be designed based on the current physics and engineering basis with a reasonable running cost (~5B Yen/year). Although the achievable neutron flux is 2–3 orders lower than that of accelerator driven neutron sources, tokamak and helical neutron sources can provide a much larger irradiation area for the test of large components. Laser neutron sources have both high operability and tritium breeding capacity. These reactor-based neutron sources also serve as an integrated test bed of the entire reactor system.

Keywords: Reactor-based volumetric neutron source, Tokamak, Helical, Laser

1. Introduction

To realise a D-T fusion power plant, an irradiation test of the reactor materials and components by 14 MeV fusion fast neutrons is strongly desired. At present, accelerator driven neutron sources using the d-Li reaction (e.g., the A-FNS [1] by Japan, the IFMIF-DONES by the EU [2]) have been planned because these concepts have a high cost performance in terms of the maximum available neutron flux. For example, the A-FNS can achieve a neutron production rate of 6.8×10^{16} n/s and the neutron flux in the high irradiation region is $>10^{18}$ n/m^2/s, which corresponds to >20 dpa/year for reduced-activation ferritic/martensitic (RAFM) steel. A concern is that the high irradiation volume is quite limited (~0.5 L). The neutron spectrum is also different from the actual fusion environment and varies with the position. The development of laser driven neutron sources using laser accelerated ion beams is in progress. Such laser driven neutron sources have a potential to achieve a neutron flux comparable to that of accelerator driven neutron sources in much more compact devices [3]. However, the laser driven neutron sources have the same issues as accelerator-driven neutron sources, such as

limited irradiation volume and anisotropy of the neutron spectrum.

In contrast, reactor-based volumetric neutron sources (VNS) can provide a larger irradiation volume with a monoenergetic and a homogenous neutron field. Even if the neutron flux is low, such an irradiation environment is useful for the test of large components or multiple samples. These reactor-based VNS can also serve as an integration test bed of the entire reactor system. Therefore, reactor-based VNS are attractive and worth considering if they can be constructed based on current physics and engineering achievements with a reasonable running cost. In this respect, various concepts have been proposed, including spherical tokamak-based devices (ST-FNSF [4], FNS-ST and DEMO-FNS [5]), the Mirror-based Gas Dynamic Trap (GDT) [6], and so on. These activities were coordinated as an IAEA research project and summarised in the report [7]. In this study, tokamak, helical and laser reactor based VNS have been examined because sophisticated design activities and related R&D towards a commercial power plant have been conducted for these three reactor types. In Japan, the development of systems codes for these three reactor types has been advanced and the authors have conducted the work for the development or improvement of these system codes. Regarding the tokamak reactor, the systems code TPC [8] has been developed and utilised for the conceptual design of several tokamak reactor concepts, including the JA DEMO reactor [9-11]. Regarding the helical reactor, the systems code HELIOSCOPE [12] has been developed and utilised for the conceptual design of the Large Helical Device (LHD)-type helical reactor FFHR series [13, 14]. Regarding the laser reactor, the systems code SUPERFLARE has been developed and utilised for the conceptual design of the dry-wall, fast-ignition laser reactor FALCON-D [15]. This study has been conducted by making full use of these systems codes.

2. Design Prerequisites

Considering the design feasibility of the reactor-based VNS, the assumed engineering and physics design parameters in this study were basically limited to those already achieved by the device in operation or expected for the device under construction. Regarding the tokamak reactor-based VNS, physics conditions that are assumed in a fully inductive operation scenario in ITER and the technological basis for the JT-60SA are considered. Regarding helical and laser reactor-based VNS, the achievements in the LHD and GEKKO-XII are considered, respectively. These conditions will be described in more detail in the next section. In addition to these physics and engineering design constraints, availability and running cost are other important factors to discuss the design feasibility. In this study, the following design prerequisites are taken into account.

Regarding the tokamak and helical reactor-based VNS, the use of superconducting coils is assumed to achieve a steady-state operation. Therefore, the installation of a neutron shield with a sufficient thickness is required to suppress the nuclear heating on the superconducting coils. Regarding the plasma heating method, the neutral beam injection (NBI) system is considered to enhance the neutron generation rate through the beam-bulk fusion reaction. The beam acceleration energy of NBI is limited to ~100 keV by considering the possibility of the use of positive ion-based NBI, which is expected to be easier to realise a stable and steady-state operation. Regarding the laser reactor-based VNS, a laser with a high pulse energy and a high repetition rate (10 J/100 Hz) has become available by the recent progress in the development of the diode-pumped solid state laser module. The 10 kJ/100 Hz system can be realised by arraying them. In this study, the 10 kJ/100 Hz laser system is assumed but the actual repetition rate is set to 10 Hz in consideration of the injection capability of the target, based on present pellet injection development status [16].

In order to reduce the construction cost, the size and the magnetic field strength of the magnetic confinement system should to be reduced as low as possible. In such a compact reactor, achievement of electricity self-sufficiency is hardly expected. Therefore, electricity charges will account for a large fraction of the running cost. Considering the electricity charge for a large consumer of ~2,000 Yen/month plus ~15 Yen/kWh in Japan, the annual electricity cost for a steady-state operation will be 0.5B Yen/MW/year. In this study, the acceptable annual electricity charge for the NBI system or the laser system is assumed to be up to 5B Yen. The efficiency of NBI system and laser system are expected to be ~50% and ~2.5%, respectively. Therefore, the allowable maximum injection power of the NBI system and the laser system will be ~5 MW and 0.25 MW, respectively. Regarding the tokamak and helical reactor-based VNS, tritium breeding and electricity generation are not considered as prerequisites because the limited space between the plasma and the superconducting coils should be used to maximize the neutron shielding performance. Therefore, the net tritium breeding ratio (TBR) and the electric output are not included in the design requirements. In order to reduce the amount of the external supply of tritium, breeding blankets are installed as long as space is available. Tritium production by DD operation is also considered.

3. Design Window Analysis

3.1 Tokamak reactor-based VNS

In the case of a tokamak reactor, the systems code TPC [17] is used for the design window analysis. Because the current version of the TPC does not handle the beam-bulk fusion reaction, the energy multiplication factor Q_{B} is estimated by a simple model [18, 19] as follows:

$$Q_{\mathrm{B}} = \frac{E_{\mathrm{fus}}}{E_{\mathrm{beam}}} n_i \int_{E_{\mathrm{th}}}^{E_{\mathrm{beam}}} \frac{\langle \sigma v \rangle_{\mathrm{B}}}{-\langle \mathrm{d}E/\mathrm{d}t \rangle} \mathrm{d}E, \quad (1)$$

where E_{fus}, E_{beam}, n_i, E_{th} and E are energy yield by the fusion reaction (17.06 MeV for D-T reaction), NBI beam acceleration energy, bulk ion density, bulk ion thermal energy, and the energy of NBI fast particles, respectively. For simplicity, temperature equality ($T_e = T_i$) is assumed and the term $\langle \mathrm{d}E/\mathrm{d}t \rangle$ is calculated using the energy relaxation time between NBI fast particles and bulk electrons. $\langle \sigma v \rangle_{\mathrm{B}}$ is the beam-bulk fusion reaction rate calculated as follows:

$$\langle \sigma v \rangle_{\mathrm{B}} = \sqrt{\frac{m_i}{2\pi k_B T_i}} \int_0^{\infty} u\sigma(u)\, \mathrm{d}u, \quad (2)$$

where m_i, k_{B}, T_i, and u are bulk ion mass, the Boltzmann constant, bulk ion temperature and relative velocity between a bulk ion and an NBI beam ion. The fusion cross-section $\sigma(u)$ is calculated by the model in ref. [20]. Figure 1 shows the dependence of the energy multiplication factor Q_{B} on bulk ion temperature calculated by eqs. (1) and (2). It was found that fusion energy equivalent to the beam energy is expected in the case of the injection of a deuterium (D) beam into pure tritium (T) plasma with the ion temperature of ~20 keV. In the case of the injection of the D beam into D-T plasma, Q_{B} becomes almost half.

The systems code TPC calculates the plasma performance from the input parameters of major radius R_0, plasma aspect ratio A_p, safety factor q_ψ, normalized beta β_N, averaged ion temperature $\langle T_i \rangle$, TF coil thickness d_{TF} and the gap between the plasma and the TF coil Δ_{TF} at the inboard side. The toroidal magnetic field strength B_{t} is calculated based on the

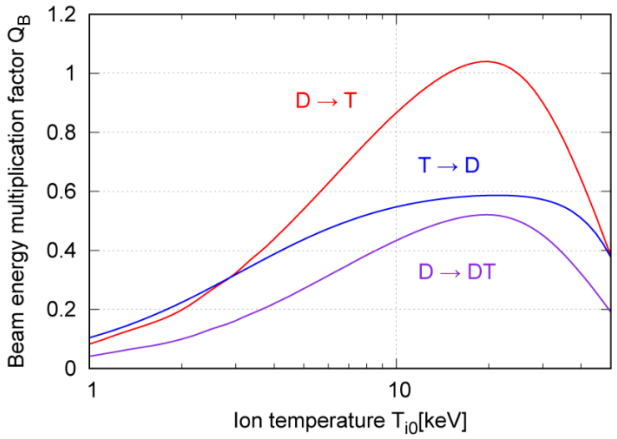

Figure 1. Beam Energy multiplication factor as a function of ion temperature in the case of the beam acceleration energy of 100 keV.

geometry of TF and CS coils by considering heat balance, electromagnetic stress and performance of the superconductor. In this study, the specification of the conductor is assumed to be the same as that of the JT-60SA: 26 kA NbTi conductor for the TF coils and 20 kA Nb_3Sn conductor for the CS coils. The CS coil radius is set to enable an inductive operation with a duration of one hour. In the case of an average neutron wall load of ~1 MW/m^2, the neutron shielding with a thickness of ~80 cm is required to sufficiently suppress the fast (> 0.1 MeV) neutron flux on the superconducting coil, if the thickness that corresponds to the one order of magnitude reduction of the fast neutron flux is 20 cm. In the case that the fusion power is ~5 MW and the major radius of R_0 ~3 m, the average neutron wall load is ~0.01 MW/m^2. Considering the use of the neutron shielding with a thickness that corresponds to the one order of magnitude reduction of the fast neutron flux, 15 cm, a neutron shielding thickness of ~30 cm is required.

Figure 2 shows the result of the design window analysis for the parameter ranges shown in Table 1. It was found that the minimum reactor size is R_0 = 3.4 m with B_{t} = 4.46 T and I_p = 4.24 MA if the physics parameters are confined to those of the ITER inductive operation scenario [21]: the Greenwald density limit ratio $n/n_{\mathrm{GW}} \leq 1$, normalized beta $\beta_N \leq 1.8$, safety factor q_ψ = 3 and confinement improvement factor to the H-mode scaling $H_H \leq 1$. In the case of the injection of the D beam into D-T plasma, fusion power by thermal fusion reaction and the beam-bulk fusion reaction are ~0.9 MW and ~2.5 MW, respectively. Therefore, the maximum achievable

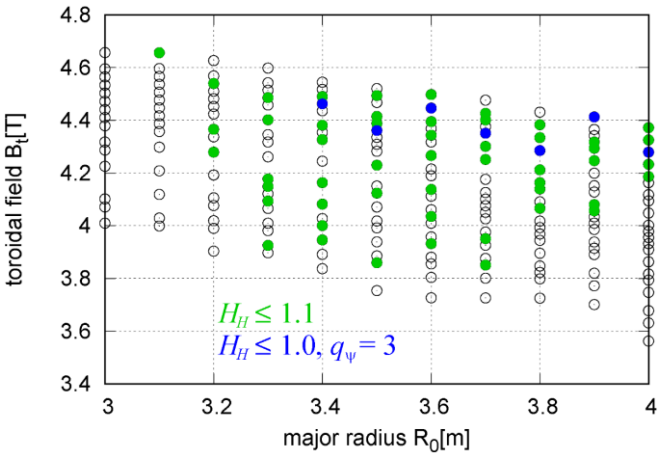

Figure 2. Result of design window analysis for tokamak reactor-based VNS.

Table 1. Parameter scan range and constraints for the Tokamak-based VNS

Major radius R_0 [m]	3.0 – 4.5
Plasma aspect ratio A_p	3 – 4
Ellipticity κ	1.7
Safety factor q_ψ	3 – 4
normalized beta β_N	1 – 1.7
averaged ion temperature $\langle T_i \rangle$ [keV]	12
TF coil thickness d_{TF} [m]	0.25 – 0.35
gap between the plasma and the TF coil Δ_{TF} [m]	0.30
NBI injection power P_{NBI} [MW]	5

fusion power is ~5 MW with the beam-bulk fusion by the injection of the D beam into T plasma. Consequently, the achievable neutron production rate is 3.6×10^{18} n/s. The neutron flux of 1.8×10^{16} n/m^2/s can be provided in an area of ~200 m^2. One of the big issues of the tokamak reactor-based VNS is its availability due to the difficulty in the steady-state current drive. Assuming a conservative value of the availability of 50%, annual neutron production will be ~4.5×10^{25}. The direct construction cost of this tokamak reactor-based VNS, estimated by the present cost model, is 300–400B Yen. Note that this cost is based on the mass unit cost of the material and the manufacturing cost of each component, facility and building for the ITER that assessed in Japan in 1997. There are several cost-increasing factors such as price and wage increase, difference in required manufacturing accuracy, and difference in safety management standards. Because the volume of the fusion island is relatively small, compared with a device that has a larger major radius such as a DEMO reactor, the plant facilities account for about half of the construction cost.

As shown in Fig. 2, the impact of the improvement of the core plasma performance on R_0 and B_t is not so large. This is because R_0 is mainly determined by the radius of the CS coil and B_t is determined by the thickness of the TF coils. Consequently, the cost performance as a VNS strongly depends on the availability of the system. The NBI power and the accompanying fusion power can be increased, keeping the same physics constraints. In order to double the NBI power while keeping the fast neutron flux on the superconducting coils, ~6 cm increase of the thickness of the neutron shielding is required. Because this increase can be realised by a slight increase of R_0 and the plasma aspect ratio, the achievable neutron flux can be increased without a big impact on the construction cost. This means that the neutron generation rate can be increased if a higher running cost is permitted.

3.2 Helical reactor-based VNS

In the case of a helical reactor, the reactor size strongly depends on the space between the plasma and the helical coils (HC). The systems code HELIOSCOPE calculates plasma performance from the input parameters of a HC major radius R_c, magnetic field strength at the centre of the HC windings B_c and the HC current density j_c. Figure 3 shows the dependence of the minimum shielding thickness and expected ion temperature on R_c and the R_c in the case of j_c = 35 A/mm^2, which is based on the LHD achievement. In typical discharges of the LHD experiment, the plasma pressure has shown the gyro-Bohm type parameter dependence [22],

$$p \propto n^{0.6} P_{abs}^{0.4} B_{ax}^{0.8}, \quad (3)$$

where n, P_{abs}, B_{ax} are the plasma density, the total absorbed power and the magnetic field strength at the magnetic axis, respectively. The critical magnetic field of an NbTi conductor is ~ 12 T and the maximum allowable magnetic field on the

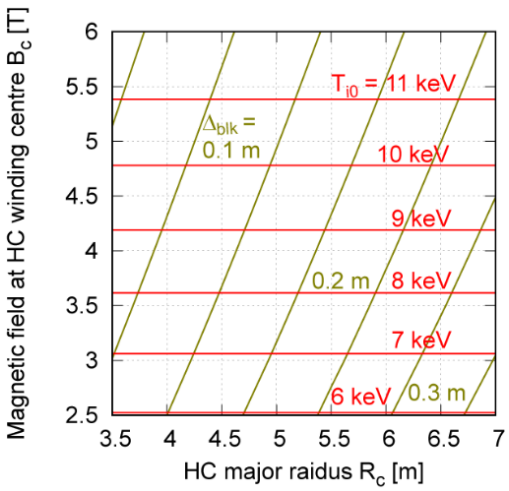

Figure 3. Result of design window analysis for the helical reactor-based VNS with the helical coil current density j_c = 35 A/mm^2 and the plasma density of 0.8×10^{19} m^{-3}.

HC is ~ 9 T. Because the maximum magnetic field on the HC is about two times larger than B_c, $B_c \leq 4$ T is required. Assuming $n = 0.8\times10^{19}$ m^{-3} and P_{abs} = 5 MW, it was found that the shielding thickness of 25 cm and ion temperature of ~8 keV can be simultaneously achieved with R_c = 6.0 m and B_c = 3.8 T. In the case of R_c = 6.0 m, the average neutron wall load is half that of the tokamak reactor-based VNS with R_0 ~ 3 m. Then the required thickness of the neutron shielding is 25 cm.

The achievable fusion power by the beam-bulk fusion reaction should be examined in more detail because a three dimensional magnetic field structure may affect the fusion reaction rate. Therefore, the radial profile of the NBI power deposition and the beam-fusion reaction rate is calculated using the FIT3D code [23], which has been developed for the analysis of the NBI heating of the LHD. In the case of a strongly NBI heated plasma with a beam-bulk fusion reaction, the plasma pressure attributed to the injected neutral beam particles and the generated alpha particles becomes high. In this study, the radial profiles of the neutral beam pressure and the alpha pressure are estimated by multiplying a constant factor to the NBI power deposition profile and the alpha particle birth profile, respectively. These factors are derived from the comparative calculation using the GNET code [24], which can calculate the pressure profile of the beam ions and alpha particles, for the device with R_c = 3.9 m and B_c = 5.7 T. The radial profiles of the bulk temperature of ions and electrons are estimated by extrapolating those of the reference LHD experimental data, based on the gyro-Bohm type parameter dependence given as eq. (3) considering the equipartition effect. In the LHD experiment, it has been observed that the energy confinement property improves by increasing the peaking factor of the heating profile [25]. On the other hand, the energy confinement property degrades with

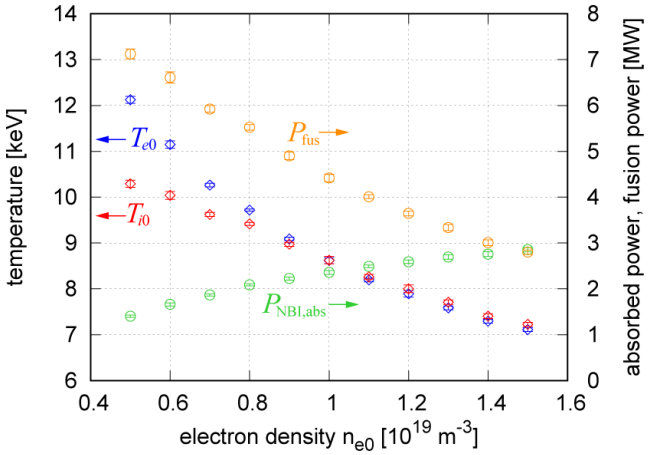

Figure 4. Dependence of electron temperature, ion temperature, absorbed NBI power and fusion power on the electron density for the helical reactor-based VNS with R_c = 6.0 m and B_c = 3.8 T.

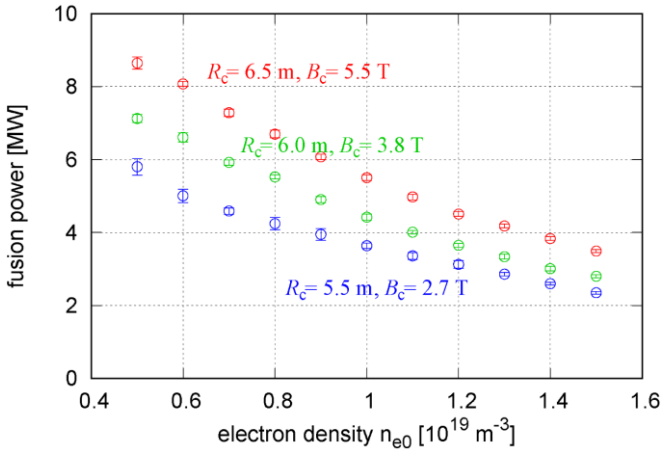

Figure 5. Dependence of the fusion power on the electron density for the helical reactor-based VNS with different R_c and B_c.

the outward shift of the magnetic axis position [26]. This degradation is mainly caused by the enhancement of the neoclassical transport due to the change in the vacuum magnetic field structure and similar degradation is expected in the case of the magnetic axis shift by the increase of the plasma pressure. In this study, these effects are taken into account. Figure 4 shows the dependence of bulk electron temperature, bulk ion temperature, absorbed NBI power and the fusion power by the beam-bulk fusion reaction on the electron density for R_c = 6.0 m and B_c = 3.8 T. It was found that the fusion power equivalent to the injected NBI power (P_{fus} ~ 5 MW) can be achieved by the injection of the D beam into T plasma at the electron density of 0.8×10^{19} m^{-3}. Although the fusion power increases with the decreasing electron density and the increasing the ion temperature, low density operation is not favourable from the viewpoint of the damage on the NBI counter wall, due to the increase of the shine-through. Figure 5 shows the dependence of fusion power for three cases of the set of the reactor size and the magnetic field strength that satisfies a neutron shield thickness of 25 cm: (R_c, B_c) = (5.5. 2.7), (6.0, 3.8) and (6.5, 5.0). It was found that the fusion power mainly depends on the magnetic field strength. The minimum magnetic field strength that can realize a fusion power of P_{fus} ~ 5 MW with the electron density of ~1.0×10^{19} m^{-3} is B_c ~ 4 T, which corresponds to R_c ~ 6 m. In the case of D the injection of the D beam into D-T plasma, the thermal fusion power is ~0.1 MW and the beam-bulk fusion power is expected to be less than half of that in the case of the injection of the D beam into T plasma. Therefore, the maximum achievable fusion power is ~5 MW in the case of the injection of the D beam into T plasma. Consequently, the achievable neutron production rate is 1.8×10^{18} n/s. The neutron flux of 4.5×10^{15} n/m^2/s can be provided in an area of ~400 m^2. Because there is no need for the plasma current drive, the requirement on the NBI system is moderated and a year-long steady-state operation is expected. Therefore the annual neutron production will be ~6.0×10^{25}. Although the major radius of the helical reactor-based VNS is about 1.7 times larger than that of the tokamak reactor-based VNS, the mass of each component is almost the same because the aspect ratio of the device is larger. The scale of the buildings and the plant facilities are also the same as those of the tokamak reactor-based VNS because the fusion output is the same. Therefore, the estimated cost of the helical reactor-based VNS is also the same as that of the tokamak reactor-based VNS: 300–400B Yen.

In the case of a helical reactor, the plasma shape is uniquely determined by the geometry of the helical coils. In order to double the NBI power, ~10% increase of R_c is required. On the other hand, if the current density of the helical coil j_c increases, R_c can be reduced while keeping the fusion power. If both j_c and B_c increases, the fusion power can be increased while keeping R_c. Consequently, the increase of j_c and B_c is the most effective way to reduce the cost performance as a VNS.

3.3 Laser reactor-based VNS

Regarding a laser reactor, the neutron yield of ~10^{13} per shot has already been achieved with the irradiating laser energy of 10 kJ, using a target design called LHART (Large High Aspect Ratio Targets) [27]. As described in the previous section, 100 Hz repetition is achievable in terms of the laser system. Assuming the repetition rate of 10 Hz based on present pellet injection development status, the achievable neutron production rate is 10^{14} n/s. The minimum chamber size is determined by the heat load limit. The maximum allowable heat load on a dry wall chamber is estimated to be 2 J/cm^2 [15]. In this case, fusion pulse energy is ~30 J and the heat load is sufficiently small if the chamber with a practical size (e.g., a diameter of > 0.1 m) is adopted. Consequently, achievable neutron flux is 8×10^{14} n/m^2/s with a spherical

chamber that has a diameter of 0.1 m (a surface area of 0.125 m^2).

The neutron yield Y_n of the compressed target with the mass density ρ and radius R is calculated by

$$Y_n = \frac{4\pi\rho R^3}{3m_{\mathrm{DT}}}\frac{\rho R}{\rho R + \xi(T)}, \quad (4)$$

$$\xi(T) = \frac{8m_{\mathrm{DT}}c_s}{\langle\sigma v\rangle_{\mathrm{DT}}} = \frac{8(m_{\mathrm{DT}}k_B T)^{0.5}}{\langle\sigma v\rangle_{\mathrm{DT}}}, \quad (5)$$

where m_{DT}, c_s and $\langle\sigma v\rangle_{\mathrm{DT}}$ are the mass of the target, ion sound velocity and the reactivity of thermal D-T fusion, respectively. In the case of a small target, $\rho R \ll \xi(T)$ and $Y_n \propto \rho^2 R^4/\xi(T)$. Assuming a homogeneous density and temperature of the compressed target for simplicity, the required laser pulse energy E_L is proportional to the total internal energy of the target: $E_L \propto (4\pi/3)\rho T R^3$. This means $Y_n \propto E_L^{4/3}$ and the neutron yield becomes 10 times larger if the laser energy is 5.5 times larger. This means both the neutron generation rate and the cost performance can be increased while increasing the laser energy and keeping the electric power consumption. Because the chamber size is relatively small, the laser system and target the factory account for the majority of the cost of the laser reactor-based VNS. The cost of the laser system is estimated to be ~100B Yen.

In the case of a laser fusion reactor, the irradiation area and the neutron flux can be flexibly varied by the chamber design. Because there is no limit on the space for blanket modules, the blanket design can be optimised for tritium breeding and a net tritium breeding ratio (TBR) > 1 can be achieved. If an increase of the running cost is permitted, the operation of multiple (up to 10) chambers is also possible by steering the laser beams. Although the duration of the operation depends on the target injection capability, a year-long operation is expected.

4. Summary

The performance of tokamak, helical and laser reactor-based volumetric neutron sources is summarised in Table 2. The performance of the A-FNS is also listed in Table 2 for comparison. Although the achievable neutron flux of the reactor-based VNS is 2–3 orders lower than that of the A-FNS, the annual neutron production of tokamak and helical reactor-based VNS is higher and the irradiation are is also much larger. The tokamak reactor-based VNS can achieve the highest neutron flux among three types of the reactor-based VNS, while it has an issue with the availability. The helical reactor-based VNS has a larger device size compared with other systems, but it has an advantage in a steady-state operation capability. Because the construction cost of the helical rector-based VNS is the same as that of the tokamak reactor-based VNS, the cost of neutrons can be lowest among the three reactor types. Although the neutron generation rate of the laser reactor-based VNS is much lower than other systems, it has a high flexibility in the operation, resulting from a high degree of freedom in the design of both the reactor chamber and the laser system. The construction cost of the laser reactor-based VNS is also much lower than the other reactor types. Although the 'pure' cost of neutrons is the highest, the laser reactor-based VNS has a unique value of the high operational flexibility and the possibility of the tritium breeding.

It was concluded that the reactor-based VNS can be designed based on the present physics and engineering basis with a much smaller device size compared with that of the conceptual design, which aims at the realisation of electric power generation for each type reactor [14,28,29]. Therefore, these reactor-based VNS can provide the experimental environment of burning plasma and the test environment of the entire reactor system (e.g., the plasma exhaust system,

Table 2. Comparison of the performance of Tokamak, Helical and Laser reactor as a neutron source

	Tokamak	Helical	Laser	A-FNS
Device size [m]	3.4 (major radius)	6.5 (major radius)	> 0.05 (chamber radius)	–
Electric power requirement [MW]	10 (for NBI)	10 (for NBI)	4 (for laser)	10 (for beam)
Neutron generation rate [n/s]	1.8×10^{18}	1.8×10^{18}	1×10^{14}	6.8×10^{16}
Neutron flux [$n/m^2/s$]	9.0×10^{15}	4.5×10^{15}	$< 8.0\times10^{14}$	$> 10^{18}$ (high) $\sim10^{17}$ (low)
Irradiation area [m^2]	~200	~400	> 0.125	~0.5 (high) ~4 (low)
Annual neutron production	$\sim3\times10^{25}$	$\sim6\times10^{25}$	$\sim3\times10^{21}$	$\sim2\times10^{24}$
Estimated construction cost [B Yen]	300–400	300–400	~100	N/A
Issues towards the increase of the neutron generation rate	Increase of the availability	Increase of the HC current and the current density	Increase of the laser energy and the repetition rate	–

tritium processing system and heat recovery system) at an earlier stage with a lower cost. The clarified issues that are needed to increase the neutron generation rate are directly related to the issues of the reduction of the cost and the developmental risks for a future fusion power plant. Therefore, these reactor-based VNS can also provide an opportunity to demonstrate several advanced physics and engineering concepts to solve such developmental issues for a future fusion power plant.

Acknowledgements

The work was supported by the budgets of NIFS11UFFF011 of the National Institute for Fusion Science and BA DEMO Design collaboration Research of the National Institutes for Quantum and Radiological Science and Technology (QST). The authors appreciate Prof. S. Murakami and Mr. Y. Shoji at Kyoto University for their great contribution in the GNET calculation for the helical reactor-based VNS. The authors also appreciate the member of the Reactor System Group of the QST for their valuable advice.

References

[1] Nishitani T. *et al* 2015 *Fusion Sci. Technol.* **68** 326
[2] Ibarra A. *et al* 2018 *Nucl. Fusion* **58** 105002
[3] Alvarez J. *et al* 2014 *Physics Procidea* **60** 29
[4] Menard J.E. *et al* 2016 *Nucl. Fusion* **56** 106023
[5] Kuteev B.V. *et al* 2015 *Nucl. Fusion* **55** 073035
[6] Anikeev A.V. *et al* 2016 *AIP Conf. Proc.* **1771** 099001
[7] International Atomic Energy Agency 2019 Conceptual Development of Steady State Compact Fusion Neutron Sources *IAEA-TECDOC-1875* Vienna
[8] Fujieda H., Murakami Y., Sugihara M. 1992 Tokamak plasma power balance calculation code (TPC code) outline and operations manual *JAERI-M-92-178* 92 [in Japanese]
[9] Tobita K. *et al* 2007 *Nucl. Fusion **47*** 829
[10] Goto T. *et al* 2014 *Plasma Fusion Res.* **9** 3405140.
[11] Tobita K *et al* 2018 *Fusion Sci. Technol. **75*** 372
[12] Goto T. *et al* 2011 *Nucl. Fusion* **51** 083045
[13] Sagara A. *et al* 2017 *Nucl. Fusion **57*** 086046
[14] Goto T. *et al* 2019 *Nucl. Fusion **59*** 076030
[15] Goto T. *et al* 2009 *Nucl. Fusion* **49** 075006
[16] Mori Y. *et al* 2019 *Fusion Sci. Technol.* **75** 36
[17] Nakamura M. *et al* 2012 *Fusion Eng. Des.* **87** 864
[18] Niikura S., Nagami M. 1988 *Fusion Eng. Des.* **6** 109
[19] Niikura S., Nagami M., Horiike H. 1988 *Fusion Eng. Des.* **6** 181
[20] Bosch H.S., Hale G.M., 1992 *Nucl. Fusion* **32** 611
[21] Shimada M. *et al* 2007 *Nucl. Fusion* **47** S1
[22] Miyazawa J. *et al* 2011 *Fusion Eng. Des.* **86** 2879
[23] Murakami S., Nakajima N., Okamoto M. 1995 *Fusion Technol.* **27** 256
[24] Murakami S. *et al* 2004 *Fusion Sci. Technol.* **46** 241
[25] Miyazawa J. *et al* 2012 *Nucl. Fusion* **52** 123007
[26] Yamada H. *et al* 2005 *Nucl. Fusion* **45** 1684
[27] Takabe H. *et al* 1988 *Phys. Fluids* **31** 2884
[28] Tobita K. *et al* 2019 *Fusion Sci. Technol.* **75** 372
[29] Norimatsu T. *et al* 2017 *Nucl. Fusion* **57** 116040